

Nonlinear generation and manipulation of Airy beams

Tal Ellenbogen*, Noa Voloch-Bloch, Ayelet Ganany-Padowicz and Ady Arie*

Recently, the first experimental observation of a new class of non-diffracting optical beams that freely accelerate in space was reported¹. These so-called Airy beams were shown to be useful for optical micro-manipulation of small particles² and for the generation of curved plasma channels in air³. To date, these beams have been generated only by using linear diffractive elements. Here, we show a new way of generating Airy beams by using three-wave mixing processes, which occur in asymmetric nonlinear photonic crystals. We experimentally generated a second-harmonic Airy beam and examined the tuning properties of the nonlinear interaction and propagation dynamics of the pump and second-harmonic output beams. This nonlinear generation process enables Airy beams to be obtained at new wavelengths, and opens up new possibilities for all-optical switching and manipulation of Airy beams.

Airy wavepackets were first predicted by Berry and Balazs⁴ in the context of quantum mechanics as a free-particle solution of the Schrödinger equation. The envelope of these wavepackets is described by Airy functions, centred around a parabolic trajectory in space. The Airy wavepacket is the only non-spreading solution in one dimension. Its unique acceleration property is attributed to the caustic of the wavepacket and not to the centre of mass, so the acceleration does not contradict Ehrenfest's theorem.

The theoretical background to the generation of optical Airy beams was only recently presented⁵, followed soon by their first experimental observation¹. The ballistic dynamics of the beams, together with their facility to bypass obstacles, were examined⁶. Their special self-healing properties, that is, self-restoration of their canonical form after passing small obstacles, have been theoretically and experimentally demonstrated^{2,7}. The dynamics of the first and second moments of these beams under different excitation parameters have also been studied⁸, and it has been shown that, according to Ehrenfest's theorem, the centre of mass moves in a straight line but the local features of the beam show a nonlinear lateral shift. It has also been shown that the linear and angular momentum of these beams change during propagation, and the total momentum and energy are conserved⁹.

To date, all studies have examined Airy beams generated by linear diffractive elements. In this work we investigate a novel type of Airy beams generated by three-wave mixing (TWM) processes, taking place in an asymmetrically modulated quadratic nonlinear optical media. The asymmetric structure induces a cubic phase front to the generated TWM output, for which the Fourier transform is an accelerating Airy beam¹.

Quasi-phase matching (QPM) in quadratic nonlinear photonic crystals^{10,11} has attracted a great deal of interest in recent years, mainly due to the major improvements in poling technology that have enabled us diverse types of one- and two-dimensional nonlinear structures^{12–14} with sub-micrometre resolution to be both designed and engineered¹⁵. The generation of Airy beams by

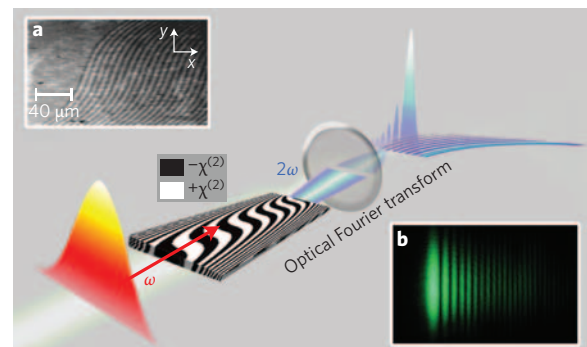


Figure 1 | Nonlinear generation of Airy beams. A Gaussian pump is converted to a second-harmonic Airy beam in an asymmetric nonlinear photonic crystal. ω is the angular frequency of the Gaussian pump beam. **a**, Microscope photograph of the C⁻ facet of the quadratic crystal, after selective etching (which reveals the inverted domain pattern). The x - and y -axes were rescaled for viewing purposes and are not comparable. **b**, Profile photograph of the green second-harmonic Airy beam.

quadratic nonlinear processes opens up new possibilities to control and manipulate their properties^{16,17}.

To generate the Airy beam we designed and fabricated an asymmetric quadratic nonlinear photonic structure with the following space-dependent quadratic nonlinear coefficient:

$$\chi^{(2)}(x, y) = d_{ij} \text{sign}[\cos(2\pi f_x x + f_c y^3)] \quad (1)$$

where d_{ij} is an element of the quadratic susceptibility $\chi^{(2)}$ tensor, f_x is the spatial frequency of the modulation in the beam's propagation direction, and f_c represents the strength of the cubic modulation in the transverse direction. An illustration of the structure and the unique conversion process is shown in Fig. 1. This binary modulation function can be expanded to a series of oscillating terms with a dominant first-order term equal to $(2/\pi) \exp[\pm i(2\pi f_x x + f_c y^3)]$.

For simplicity we consider a two-dimensional second-harmonic generation (SHG) problem with a plane pump wave that propagates in the x -direction, and generation of a collinear second-harmonic wave with an arbitrary envelope as follows:

$$E_1(x, y) = A_1 e^{ik_1 x}, \quad E_2(x, y) = A_2(x, y) e^{ik_2 x} \quad (2)$$

where A_1 and k_1 (A_2 and k_2) are the amplitude and wavevector of the first-harmonic (and second-harmonic) wave, respectively. By inserting the first-order term of the structure to the nonlinear wave equation we obtain

$$\nabla^2 A_2(x, y) + k_2^2 A_2(x, y) = -CA_1^2 e^{i(2k_1 - k_2 + 2\pi f_x)x + if_c y^3} \quad (3)$$

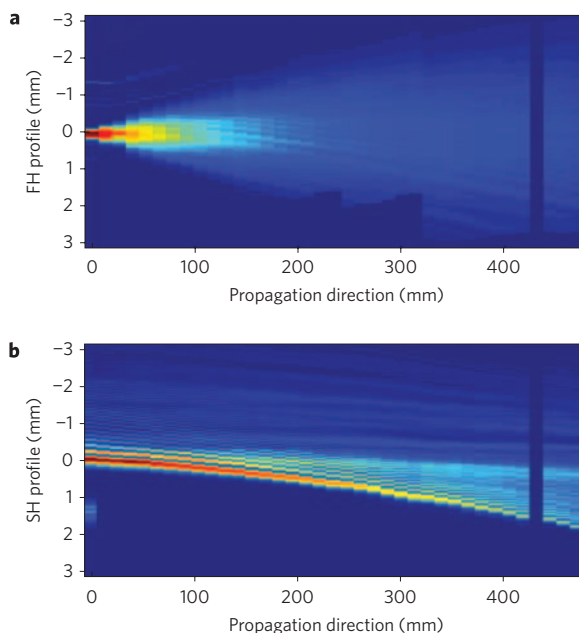


Figure 2 | Recorded propagation dynamics of the optically Fourier transformed output beams. a, Output first-harmonic (FH) pump beam. **b,** Output second-harmonic (SH) Airy beam.

where C is a nonlinear coupling coefficient. The right-hand side of this equation is the nonlinear polarization source. In collinear QPM conditions, the difference between the wavevectors of the second-harmonic and fundamental waves satisfies a momentum conservation law, $k_2 - 2k_1 = 2\pi f_x$, so the polarization source oscillations in the propagation direction are reduced and a build-up of a second-harmonic wave with a cubic phase front occurs that results from the transverse component of the polarization source term. Performing an optical Fourier transform, for example, using a lens, on the TWM output (second-harmonic in this case), results in the Airy beam^{1,5}.

We fabricated the suggested structure by two-dimensional poling of a stoichiometric lithium tantalate (SLT) nonlinear crystal (see Methods) and generated an Airy beam at the second-harmonic of a single-mode Gaussian Nd:YLF pump. A microscope photograph of the modulated nonlinear crystal after selective etching and a photograph of the green second-harmonic Airy beam profile at the far field are shown in Fig. 1, insets (a) and (b). Using a pump wave with 3.6 kW peak power we measured a second-harmonic wave with a peak power of 42 W, giving an internal conversion efficiency (without Fresnel reflections at the crystal facets) of $8.2 \times 10^{-6} \text{ W}^{-1}$. In addition, we performed an optical Fourier transform to the output of the nonlinear photonic crystal, using a lens of 100 mm focal length, and recorded the propagation dynamics of the Fourier transformed pump and second-harmonic waves, as shown in Fig. 2 (see Methods).

The output pump wave has Gaussian beam propagation dynamics with slight intensity modulations that might be caused by small linear variations in the crystal due to the poling process. The output second-harmonic beam shows the propagation dynamics of a truncated Airy beam, that is, nearly non-diffracting and freely accelerating to one side. The size of the first lobe at the focal point of the lens was $147 \mu\text{m}$.

The measured temperature tuning properties of the nonlinear interaction were compared to a split-step Fourier numerical simulation (see Methods and Fig. 3). The maximum conversion efficiency achieved by this structure was calculated to be ~ 0.9 of the maximum conversion efficiency achieved by a conventional one-dimensional

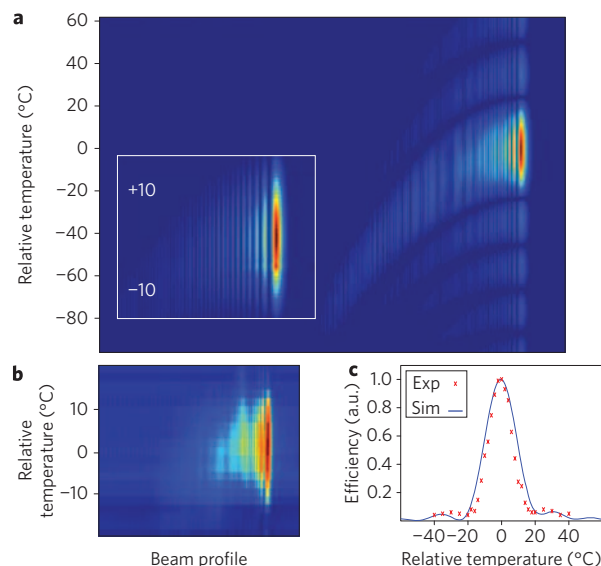


Figure 3 | Temperature tuning of the nonlinear interaction. a, Simulation of the second-harmonic beam profile (absolute amplitude values) as a function of the crystal temperature relative to phase matching point. Inset: main lobe intensity pattern. **b,** Experimental results for main lobe intensity pattern at the far field versus temperature. **c,** Simulation and experimental curves of doubling efficiency versus temperature.

periodically poled structure under the same experimental configuration. The inset shows the intensity pattern of the main phase matching lobe versus the temperature of the crystal, and Fig. 3b shows the experimental results. Note that for different phase matching conditions we obtain beams with slightly different profiles. This affects the propagation dynamics of the different output beams, as we discuss in the next paragraph. Figure 3c shows the numerical and experimental efficiency tuning curves, which are similar in shape to conventional temperature tuning curves^{10,12}. The temperature of maximum intensity was $157 \text{ }^\circ\text{C}$ in the simulation and $120 \text{ }^\circ\text{C}$ in the experiment, possibly resulting from slight inaccuracies in the dispersion equation. Nevertheless, there is good agreement between the simulated and measured tuning properties.

The nonlinear response provides new possibilities for manipulating and controlling Airy beams that cannot be achieved using linear optics. One option, shown in Fig. 4, is all-optical shaping of the caustic of the Airy beam. We simulated the propagation properties of the second-harmonic output at different phase-matching conditions, that is, different temperatures or pump wavelengths and show output results for values that are in the main phase-matching lobe shown in Fig. 3. It is demonstrated that the caustic property of Airy beams is maintained even outside phase-matching conditions; however, for different phase-matching conditions the output beam peaks at different places along the parabolic trajectory. The peak intensity values for Fig. 4a–f with respect to a phase-matched interaction are 0.05, 0.57, 1, 0.5, 0.21 and 0.12. Shaping of the caustic by changing the phase-matching conditions of the crystal is a unique property of the generation of Airy beams using nonlinear photonic structures and could be applied in fluidic micro-manipulation² and in the generation of curved plasma channels³.

Another application of the nonlinear response is to all-optically control the acceleration direction of the beam by relying on the physical difference between up-conversion and down-conversion processes. The phase mismatch values for up-conversion and down-conversion processes that involve the same three waves are opposite, so phase-matching terms with opposite signs are required by the nonlinear structure. This idea was proposed for switching the

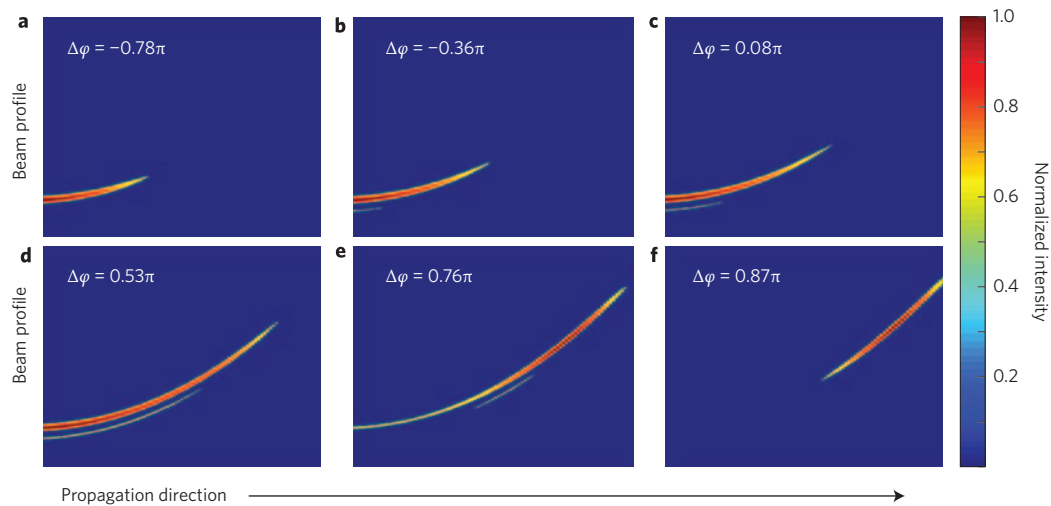


Figure 4 | Shaping the caustic of the generated Airy wavepacket by changing phase-matching conditions ($\Delta\varphi = \Delta kl/2$). The full intensity profile of the different panels resembles an Airy beam propagation profile; however, we have eliminated all values lower than half maximum values for viewing purposes. The left side of each panel is the origin of the Airy beam that propagates to the right. **a**, $\Delta\varphi = -0.78\pi$; **b**, $\Delta\varphi = -0.36\pi$; **c**, $\Delta\varphi = 0.08\pi$; **d**, $\Delta\varphi = 0.53\pi$; **e**, $\Delta\varphi = 0.76\pi$; **f**, $\Delta\varphi = 0.87\pi$.

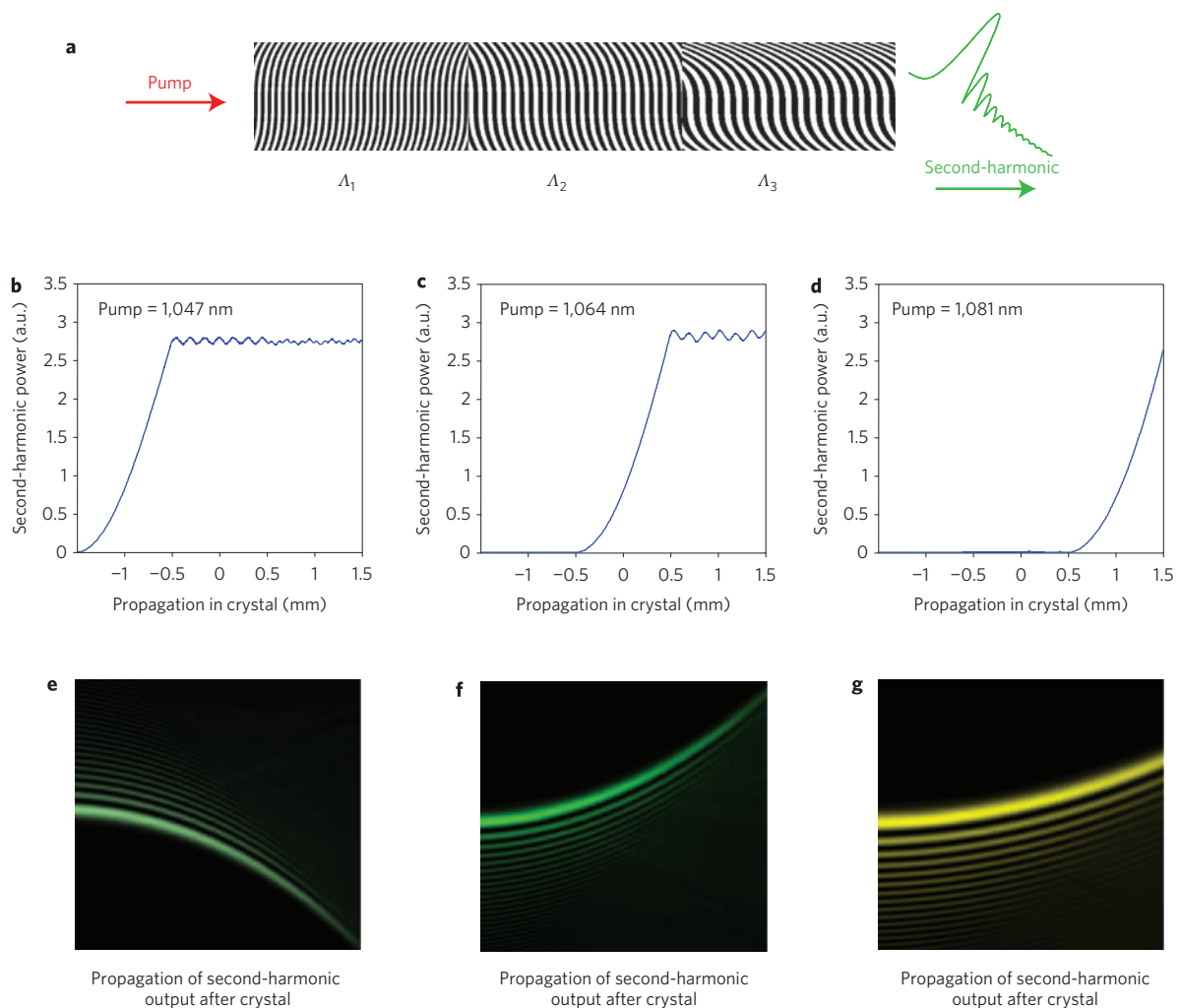


Figure 5 | All-optical control of the Airy beam's acceleration properties using cascaded nonlinear structures with different periods in the propagation direction. **a**, Illustration of the simulated structure in SLT crystal, where Λ is the poling period of each subsection of the structure. In the simulations we used $\Lambda_1 = 7.38 \mu\text{m}$, $\Lambda_2 = 7.75 \mu\text{m}$ and $\Lambda_3 = 8.12 \mu\text{m}$. **b-d**, Second-harmonic build-up in the crystal for different pump wavelengths and **e-g**, Respective output beams at the second-harmonic.

optical helicity of nonlinearly generated optical vortex beams¹⁸. By examining the polarization source in equation (3) under collinear QPM conditions in these two cases we obtain

$$S^{\text{NL}} = -C_1 e^{\pm if_c y^3} \quad (4)$$

where S^{NL} is the phase-matched nonlinear source and C_1 includes also the amplitudes of the generating waves. Switching from one process to another by choosing proper pump beams that satisfy the corresponding QPM conditions will change the sign of the effective cubic phase parameter f_c and will therefore generate an Airy beam with an opposite acceleration direction. All-optical control of the acceleration of the Airy beam can also be achieved by using cascaded structures with different cubic phase parameter and slightly different QPM conditions. Slight changes in the wavelengths of the pump beams can control the origin of the generated Airy beam and the acceleration, as illustrated in Fig. 5.

In conclusion, we have extended the idea of linear generation of Airy beams to nonlinear quadratic crystals and demonstrated experimentally, for the first time, the generation of an Airy beam at the second harmonic of a Gaussian pump laser. Our method allows the creation of Airy beams at new wavelengths and high intensities that are not supported by conventional methods. Other possibilities for obtaining Airy beams at new wavelengths include using nonlinear mode conversion¹⁹ or performing the nonlinear wave mixing of Airy beams at the Fourier plane, which will preserve the cubic phase of the interaction. In addition to the experimental realization of an Airy beam by TWM, we have shown by simulations that the caustic property of the wavepacket is maintained even for non-phase-matched interactions. Furthermore, we have demonstrated that the nonlinear generation of Airy beams allows all-optical control of the caustic and the acceleration properties of the beams. The nonlinear generation of Airy beams may also enable Airy beams to be parametrically amplified and may be useful in new quantum optics applications based on spontaneous parametric down-conversion. The idea presented here can be extended to other fields that make use of the QPM technique, for example, to generate and control extreme ultraviolet Airy beams by quasi-phase-matched high harmonic generation.

Methods

Fabrication of the crystal. We have used a conventional fabrication technique for the poling process^{17,20}. The modulation period in the propagation direction $1/f_x$ was $7.38 \mu\text{m}$ and the cubic modulation coefficient f_c was $1.9 \times 10^{-7} \mu\text{m}^{-3}$. The size of the modulated channel was $1 \times 1 \text{mm}^2$. We weakly focused the pump beam to the modulated crystal with waist radii of ~ 700 and $\sim 45 \mu\text{m}$ in the crystallographic y - and z -directions, respectively. The maximum value of cubic coefficient for a fixed channel width and fixed $1/f_x$ value is limited by the minimum domain size possible. Using state-of-the-art poling technology¹⁵ we can achieve sub-micrometre domain resolution, which in our configuration will enable us to obtain $f_c = 123 \times 10^{-7} \mu\text{m}^{-3}$ —two orders of magnitude larger.

Recording the propagation dynamics and temperature dependence. We placed a charge-coupled device camera after the focal spot of the lens and captured either the pump or second-harmonic intensity distributions (using appropriate bandpass filters) every 0.5 inches. From the photographs we derived the intensity profiles of the pump and second-harmonic waves. We used the straight trajectory of the pump to correct small lateral misalignments of the camera at different places along the trail. These profile measurements were used to produce Fig. 2.

To produce Fig. 3b we captured the far-field output of the crystal for different temperatures and derived the intensity profiles.

Numerical simulation. We simulated the nonlinear interaction using a split-step Fourier method²¹. We divided the modulated crystal into slabs of $2 \mu\text{m}$ thickness, and convolved in each slab the generated nonlinear source with the impulse response of a free-space slab. To examine the propagation dynamics of the output we calculated its Fourier transform (as was done in the experiments using a lens) and propagated the transformed output in free space.

Received 5 January 2009; accepted 13 May 2009;
published online 21 June 2009

References

- Siviloglou, G. A., Broky, J., Dogariu, A. & Christodoulides, D. N. Observation of accelerating Airy beams. *Phys. Rev. Lett.* **99**, 213901 (2007).
- Baumgartl, J., Mazilu, M. & Dholakia, K. Optically mediated particle clearing using Airy wavepackets. *Nature Photon.* **2**, 675–678 (2008).
- Polynkin, P., Kolesik, M., Moloney, J. V., Siviloglou, G. A. & Christodoulides, D. N. Curved plasma channel generation using ultraintense Airy beams. *Science* **324**, 229–232 (2009).
- Berry, M. V. & Balazs, N. L. Nonspreading wave packets. *Am. J. Phys.* **47**, 264–267 (1979).
- Siviloglou, G. A. & Christodoulides, D. N. Accelerating finite energy Airy beams. *Opt. Lett.* **32**, 979–981 (2007).
- Siviloglou, G. A., Broky, J., Dogariu, A. & Christodoulides, D. N. Ballistic dynamics of Airy beams. *Opt. Lett.* **33**, 207–209 (2008).
- Broky, J., Siviloglou, G. A., Dogariu, A. & Christodoulides, D. N. Self-healing properties of optical Airy beams. *Opt. Express* **16**, 12880–12891 (2008).
- Besieris, I. M. & Shaarawi, A. M. A note on an accelerating finite energy Airy beam. *Opt. Lett.* **32**, 2447–2449 (2007).
- Sztul, H. I. & Alfano, R. R. The Poynting vector and angular momentum of Airy beams. *Opt. Express* **16**, 9411–9416 (2008).
- Fejer, M. M., Magel, G. A., Jundt, D. H. & Byer, R. L. Quasi-phase-matched second harmonic generation: tuning and tolerances. *IEEE J. Quantum Electron.* **28**, 2631–2654 (1992).
- Berger, V. Nonlinear photonic crystals. *Phys. Rev. Lett.* **81**, 4136–4139 (1998).
- Broderick, N. G. R., Ross, G. W., Offerhaus, H. L., Richardson, D. J. & Hanna, D. C. Hexagonally poled lithium niobate: a two-dimensional nonlinear photonic crystal. *Phys. Rev. Lett.* **84**, 4345–4348 (2000).
- Arie, A., Bahabad, A. & Habshoosh, N. Nonlinear interactions in periodic and quasi-periodic nonlinear photonic crystals, in *Ferroelectric Crystals for Photonic Applications* (eds Ferraro, P., Grilli, S. & De Natale, P.) Ch. 10, 259–284 (Springer Verlag, 2009).
- Kasimov, D. *et al.* Annular symmetry nonlinear frequency converters. *Opt. Express* **14**, 9371–9376 (2006).
- Canalias, C. & Pasiskevicius, V. Mirrorless optical parametric oscillator. *Nature Photon.* **1**, 459–462 (2007).
- Konig, F., Mason, E. J., Wong, F. N. C. & Albota, M. A. Efficient and spectrally bright source of polarization-entangled photons. *Phys. Rev. A* **71**, 033805 (2005).
- Ellenbogen, T., Ganany-Padowicz, A. & Arie, A. Nonlinear photonic structures for all-optical deflection. *Opt. Express* **16**, 3077–3082 (2008).
- Bahabad, A. & Arie, A. Generation of optical vortex beam by nonlinear wave mixing. *Opt. Express* **15**, 17619–17624 (2007).
- Ellenbogen, T., Dolev, I. & Arie, A. Mode conversion in quadratic nonlinear crystals. *Opt. Lett.* **33**, 1207–1209 (2008).
- Furukawa, Y., Kitamura, K., Suzuki, E. & Niwa, K. Stoichiometric LiTaO₃ single crystal growth by double-crucible Czochralski method using automatic powder supply system. *J. Cryst. Growth* **197**, 889–895 (1999).
- Agrawal, G. P. *Nonlinear Fiber Optics* (Academic Press, 1995).

Acknowledgements

T.E. thanks Y. Sivan for fruitful discussions. This work was supported by the Israeli Science Foundation, grant no. 960/05 and by the Israeli Ministry of Science, Culture and Sport.

Additional information

Reprints and permission information is available online at <http://npg.nature.com/reprintsandpermissions/>. Correspondence and requests for materials should be addressed to T.E. and A.A.